Laser Nd:YAG Surface Hardening to Improve the Durability of Steel Components

Huan Thanh Nguyen
University of Economics–Technology for Industries, Hanoi, Vietnam
nthuan@uneti.edu.vn (corresponding author)

Received: 1 September 2025 | Revised: 16 September 2025 | Accepted: 27 September 2025

 DOI: https://doi.org/10.48084/etasr.14455

ABSTRACT

Improving the surface hardness of parts made from metal materials is a crucial factor in enhancing the durability and lifespan of products. Surface hardening is a heat treatment method that uses various heat sources (oxy-acetylene, plasma, high-frequency induction, laser, etc.) to heat the surface of the part to the phase transformation temperature, followed by rapid cooling to create a hard, wear-resistant surface layer. This study investigates the effect of key technological parameters, including laser power, laser spot diameter on the workpiece surface, and laser head movement speed, on the surface hardness of parts during the laser hardening process of 9XC steel using an ND: YAG laser. The findings show that the laser spot diameter has the most significant impact on the surface hardness of the workpiece (42.8%), followed by laser power (31.4%) and laser head speed (25.4%). These insights enable the selection of suitable technological parameters to enhance product quality, increase machining productivity, reduce production costs, and meet the surface hardness requirements of various components.

Keywords-component; surface hardening; laser heat treatment; technological parameters

I. INTRODUCTION

Laser technology is widely applied in industries such as healthcare, the military, and measurement. In machining, lasers are used for cutting, welding, drilling, and heating. Laser Heat Treatment (LHT) has shown clear advantages in improving surface quality, productivity, and tool life. Its effectiveness depends on material properties, laser power, and laser source type. Authors in [1, 2] focused on 3D heat transfer in LHT, especially for silicon nitride, a ceramic valued for low density, high-temperature resistance, and wear resistance. Cutting temperature plays a crucial role in LHT outcomes for such materials. More recently, alumina (Al_2O_3) has gained attention. Pfefferkorn's work highlighted LHT's ability to reduce heat-damaged surface layers [3], enhancing finish and reducing tool wear. Authors in [4] also reported improved machinability of alumina with reduced wear and better surface quality, addressing the limitations of traditional machining. Authors in [5] showed that LHT significantly improved Waspaloy machinability, tripling surface finish quality, boosting tool life, and cutting forces by 20%. Authors in [6] showed that using a 15kW CO_2 laser on Inconel 718 revealed that higher laser power reduced cutting force, especially at lower speeds. However, due to high costs and low absorption of long-wavelength lasers like CO_2, early adoption was limited. Later, authors in [1, 7, 8] used graphite coatings to enhance absorption in Inconel 718, reducing costs and improving LHT's feasibility, potentially lowering machining expenses by up to 50%.

Authors in [9] investigated how cutting parameters, such as speed, feed, and depth, affect LHT outcomes in Inconel 718. Their results confirmed that cutting force, tool wear, surface roughness, and hardness are key indicators of machining performance. Extensive research on materials including AISI D2, graphite, AISI 4130, and white cast iron has consistently shown that LHT offers significant advantages over conventional grinding, particularly in reducing manufacturing costs and improving efficiency [10–13]. Authors in [14-24] reported notable reductions in cutting force for hardened 9XC steel, while other studies identified the influence of parameters such as laser-to-tool distance on lowering vibration, enhancing surface quality, and increasing machining efficiency. In [25], researchers examined the heat treatment of carbon steel (0.27% C; 0.84% Mn) using quenching at different cooling rates combined with tempering at various temperatures. The samples were heated to 870°C for 2 hours, then quenched in water, oil, air, or in a furnace. The water- and oil-quenched specimens were subsequently tempered at 250–550°C for 1 hour. Tensile, impact, and microscopic analyses revealed clear microstructural changes, showing that heat treatment produced a balanced combination of tensile strength and impact toughness, making the steel well-suited for structural applications.

Thus, previous studies have been focused on applying lasers for preheating to support the machining of hard-to-cut materials, or on evaluating the individual effects of technological factors on surface quality after hardening. This study focuses on assessing the simultaneous influence of technological factors on surface hardness, using an orthogonal experimental design method to establish a mathematical model of surface hardness in the laser hardening of 9XC steel with a Nd: YAG laser, as depicted in Figure 1. This model supports

the rapid adjustment of technological parameters to improve product quality and machining efficiency.

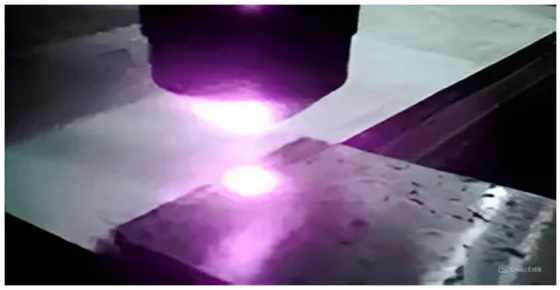

Fig. 1. Laser hardening of metal surfaces.

II. EXPERIMENTAL PROCEDURE

A. Material

The material used in this study is 9XC steel, an alloy steel, whose chemical composition as shown in Table I.

TABLE I. CHEMICAL COMPOSITION OF 9XC STEEL

C	Si	Mn	S	P	Cr	W	V	Mo
0.92	1.4	0.62	0.024	0.018	1.28	-	-	0.11

The 9XC steel has good machinability and high hardness after quenching, which can reach 55-65 HRC. This hardness allows 9XC steel to withstand wear well and has high mechanical strength, as illustrated in Table II.

TABLE II. PROPERTIES OF 9XC STEEL

Properties	Value
Young's modulus (GPa)	206
Poisson ratio	0.3
Density (kg/m^3)	7850
Yield stress (MPa)	445
Ultimate stress (MPa)	790
Elongation (%)	26
Melt temperature T_m (°C)	1460
Temperature at the critical point A_1	770
Temperature at the critical point A_3	870

In this study, the experimental samples were made from 9XC steel with dimensions of 100 mm × 60 mm ×18 mm. These samples were fabricated using the milling process.

B. Experimental Setup

To heat the surface of specimen 10, which has dimensions of 100 mm × 60 mm, the latter is placed on the workpiece holder 11, with the laser beam 9 directed at the surface. To ensure that the laser beam 9 scans the entire surface of specimen 10, the resonator chamber 6, the laser head 7, and the focusing lens 8 must move along the X-axis through the translation table 4 and along the Y-axis through the translation table 5, with an adjustable movement speed. All these components are mounted on the support table 12. On the other hand, the control cabinet 3 is used to adjust the power and movement of the laser beam, while the gas cylinder 1 and the cooling water source 2 are responsible for cooling the resonator chamber 6 and the laser head 7. All components are arranged, as depicted in the diagram in Figure 2.

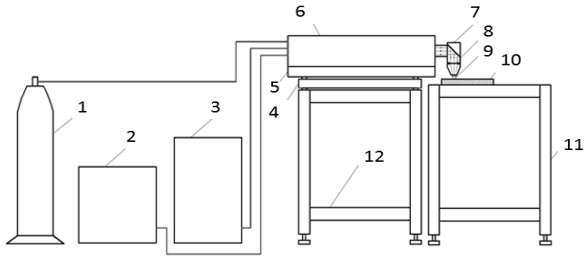

Fig. 2. Schematic of the laser hardening experimental system for 9XC steel.

C. Measuring Devices Used in Experiments

To investigate the properties and mechanics of 9XC steel material changing under the influence of ND: YAG laser, the main equipment used in the experiment includes the FieldMaster Laser Power Meter, surface temperature measuring device IR-AHS, Axio Observer D1M Microtissue Inspection Device, and Hardness measuring device. These devices are used to obtain high precision and reliability.

III. RESULTS AND DISCUSSION

The fundamental principle of laser annealing involves locally heating the material's surface to the austenitizing temperature, after which rapid self-cooling occurs as heat is conducted into the unheated core. This rapid cooling, commonly referred to as self-quenching, induces the formation of a martensitic microstructure, thereby increasing the surface hardness. Key process parameters, including laser power, scanning speed, and beam diameter, directly influence the resulting surface temperature.

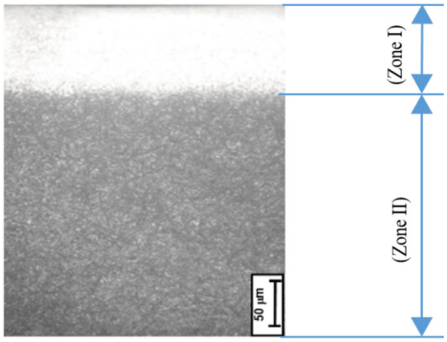

Fig. 3. Cut layer structure after heat treatment of 9XC steel by Nd: YAG laser.

Figure 3 portrays the cross-sectional microstructure of 9XC steel after Nd: YAG LHT. Zone 1, a white surface layer with high hardness, is formed when the laser heats the surface to the austenite phase; subsequent rapid cooling by Zone 2 (core) transforms it to martensite. The hardness of this layer depends on many factors; this study focuses on the effects of laser power, laser head travel speed, and beam diameter.

A. Effect of Technological Parameters on Surface Temperature

Temperature plays a critical role in determining the product quality during the steel heat treatment process. To better

understand its behavior, a detailed investigation was carried out to evaluate how different laser parameters affect the surface temperature of the workpiece. In this study, certain parameters were held constant while others were systematically varied to isolate their individual effects. To evaluate the effect of laser power on the surface temperature of the workpiece during the heat treatment process, the parameters for the laser spot diameter on the workpiece surface (D = 2.5 mm) and the laser head movement speed (v = 1.5 m/min) were kept constant. The laser power (P) was adjusted and varied from 180 W to 340 W. The results showed significant changes in the surface temperature of the workpiece as the laser power was varied, as illustrated in Figure 4.

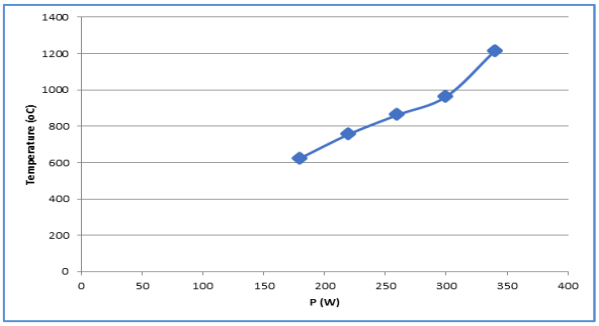

Fig. 4. Surface temperature as a function of laser power.

The parts, after being heat-treated with the laser, were cut at a right angle to the heat-treated surface, ground, and then examined for the material's microstructure, as shown in Figure 5.

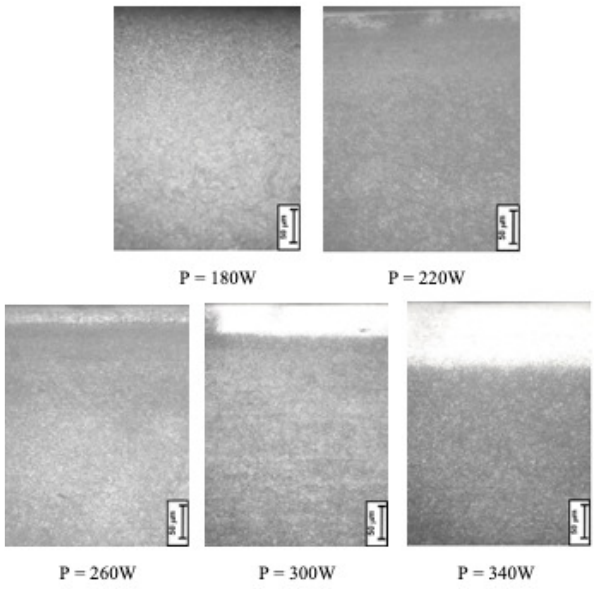

Fig. 5. Microstructure of the material after LHT with different power levels.

Based on the data displayed in Figure 5, it can be observed that with a laser power of P = 180 W, the surface temperature reaches 624°C; the microstructure of the material under the influence of the laser remains unchanged compared to the initial microstructure of the material; therefore, at a temperature of 624°C, no phase transformation from ferrite to austenite occurs. With a laser power of P = 220 W, the surface temperature reaches 756°C; at this temperature, the ferrite structure in the metal begins to transform into austenite; after rapid cooling, the austenite transforms into martensite, which has a high hardness (white grains); however, in this case, the depth of the microstructural transformation is still quite small; when using higher powers of P = 260 W, P = 300 W, and P = 340 W, the metal structure undergoes more significant changes, and the depth of transformation is greater.

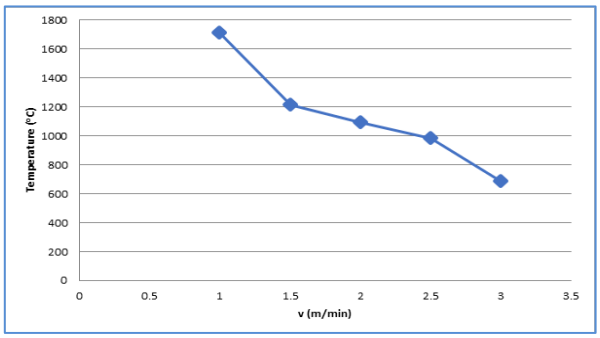

Fig. 6. Surface temperature as a function of laser head movement speed.

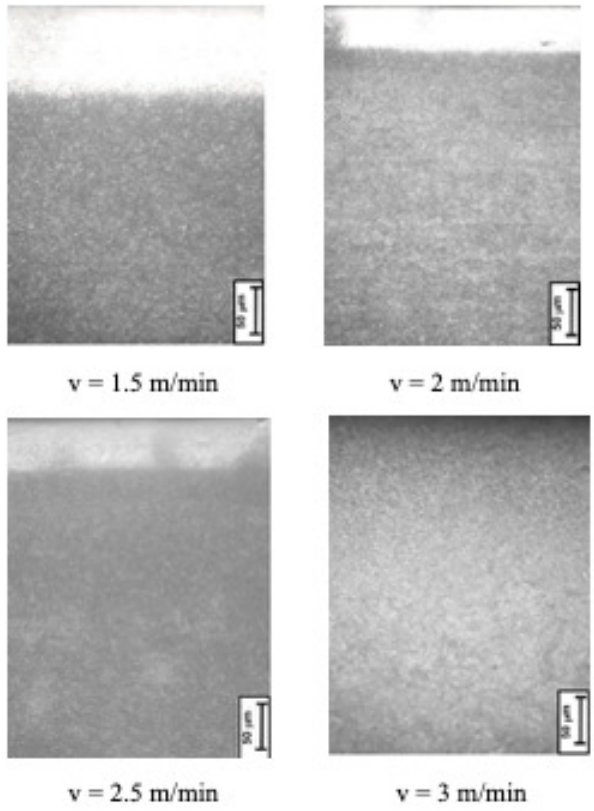

Fig. 7. Microstructure of the material after LHT with different laser head movement speeds.

Similarly, the effect of the laser head movement speed was studied while keeping the laser spot diameter on the workpiece (D = 2.5 mm) and the laser power (P = 330 W) constant. The changes in the laser head movement speed from v = 1 m/min to v = 3 m/min were investigated, resulting in significant changes in the surface temperature, as presented in Figure 6.

At v = 1 m/min, the surface temperature reaches a remarkably high value of 1708°C, resulting in the melting of the material's surface layer. In contrast, at v = 3 m/min, the surface temperature remains at a lower value of 687°C, which is not sufficient to reach the threshold needed for the material to transform into austenite, as depicted in Figure 7. To evaluate the effect of the laser spot diameter on the surface temperature of the workpiece, the laser head movement speed of v = 1.5 m/min and laser power of P = 330 W were kept constant. The laser spot diameter was varied from D = 1.5 mm to D = 3.5 mm, resulting in significant fluctuations in the surface temperature of the workpiece, as exhibited in Figure 8.

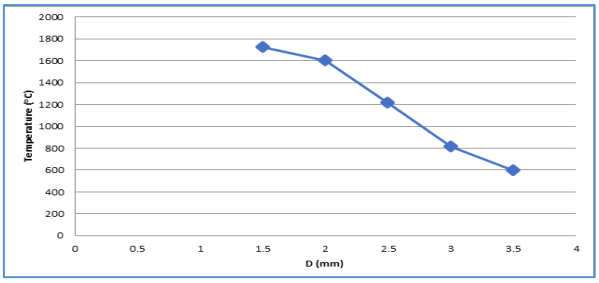

Fig. 8. Surface temperature of the workpiece as a function of laser spot diameter.

It is important that a smaller laser spot diameter (D=1.5 mm) results in a higher surface temperature of 1721°C, causing the surface material to melt. On the other hand, based on the microstructure observed after processing, with a larger laser spot diameter (D=3.5 mm), the measured surface temperature is 597°C, and the microstructure of the workpiece does not change due to the absence of the transformation from ferrite to austenite, as illustrated in Figure 9. Thus, with laser power (P) ranging from 220 W to 340 W, laser head speed (v) from 1.5 m/min to 2.5 m/min, and laser spot diameter (D) selected from 2 mm to 3 mm, the microstructure of the workpiece surface will change.

B. Building a Mathematical Model of the Influence of Technological Parameters on Surface Hardness

Table III provides the coded values and experimental values for these parameters. Each parameter is coded as -1, 0, or +1 to represent the low, medium, and high levels of the variable. The results of the experiments are outlined in Table IV, which includes the actual values of the laser power, laser head speed, laser spot diameter, and the natural logarithm of the surface hardness obtained. These experiments helped ensure the consistency and reliability of the collected data.

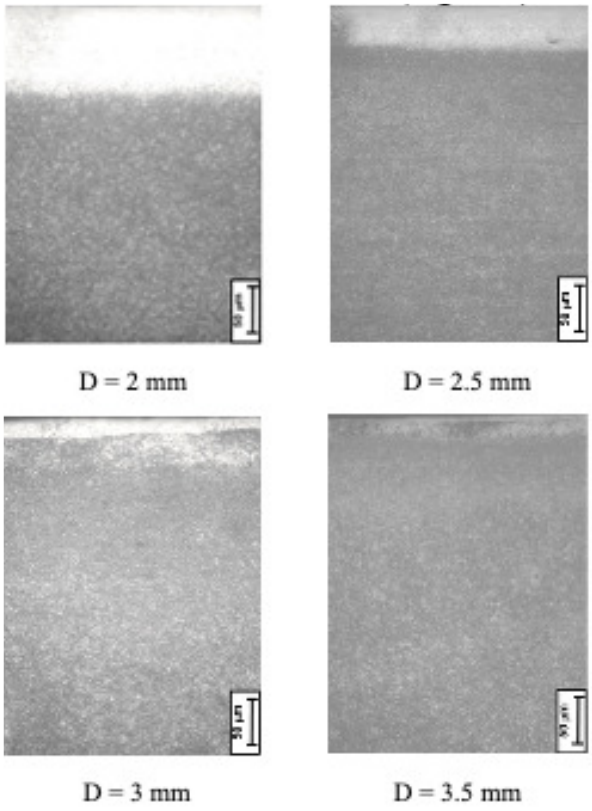

Fig. 9. Microstructure of the material after LHT with varying laser spot diameters on the workpiece surface.

TABLE III. CODED VALUES AND EXPERIMENTAL VALUES OF THE EXPERIMENTAL FACTORS

Variable symbol	Symbol	Unit	Coded value symbol		
			-1	0	+1
Laser power (P)	A	W	220	280	340
Laser head movement speed (v)	B	m/min	1.5	2	2.5
Laser spot diameter (D)	C	mm	2	2.5	3

The current study experimentally investigates the simultaneous effects of laser power (P), laser spot movement speed (v), and laser spot diameter (D) on the surface hardness of the workpiece after tempering, according to the following mathematical model:

$$H = e^{b_0} \times P^{b_1} \times v^{b_2} \times D^{b_3} \quad (1)$$

where H represents the surface hardness of the component after tempering, while b_0, b_1, b_2, and b_3 represent the dependent parameters. P, v, and D correspond to the technological parameters, and their encoded values are defined according to the detailed scheme in Table IV.

The b coefficient results using MATLAB are:

$b_0 = 0.0057$, $b_1 = 0.9461$, $b_2 = -0.5132$, and $b_3 = -1.1804$.

Therefore, the experimental problem regarding surface hardness is determined as:

$$H = 1.006 \times P^{0.9461} \times v^{-0.5132} \times D^{-1.1804} \quad (2)$$

TABLE IV. MATRIX RESULTS AND EXPERIMENTS DETERMINING SURFACE HARDNESS WITH 3 COEFFICIENTS: P, V, AND D

Trial number	Real variable			Code variable			H (HRC)
	P (W)	V (m/min)	D (mm)	A	B	C	
1	220	1.5	2	-1	-1	-1	63.2
2	220	2	2.5	-1	0	0	35.6
3	220	2.5	3	-1	+1	+1	30.0
4	280	1.5	2.5	0	-1	0	60.8
5	280	2	3	0	0	+1	33.2
6	280	2.5	2	0	+1	-1	61.6
7	340	1.5	3	+1	-1	+1	59.8
8	340	2	2	+1	0	-1	65
9	340	2.5	2.5	+1	+1	0	60

Based on the mathematical model presented in (2), the combined influence of two key parameters on surface hardness after heat treatment was analyzed. As shown in Figure 10, when the laser spot diameter is fixed at D = 2.5 mm, it is evident that a laser head speed above 2 m/min and a laser power below 260 W result in little to no change in surface hardness compared to the original material. This outcome occurs because the surface temperature generated under these conditions is insufficient to reach the austenitizing threshold required for phase transformation. In contrast, when the laser power exceeds 280 W and the laser head speed ranges from 1.5 m/min to 2.5 m/min, a significant increase in surface hardness is observed. This behavior follows the general principle that a higher laser power combined with a lower scanning speed enhances surface hardening. The results also indicate that the laser power exerts a more pronounced effect on surface hardness than the head speed, emphasizing its critical role in the process. Consequently, in practical applications, optimizing the laser head speed can help maintain consistent hardness while simultaneously improving the overall processing efficiency.

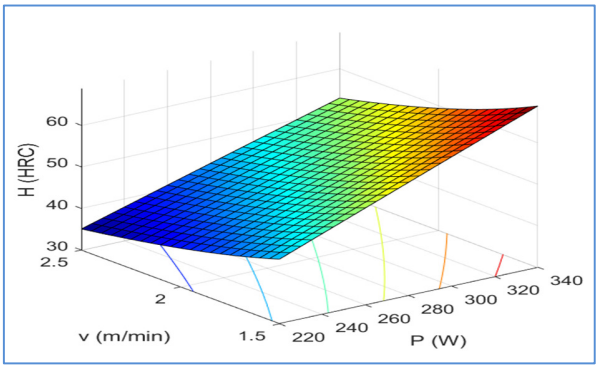

Fig. 10. The effect of P and v on the surface hardness of the part.

By keeping the laser head speed constant at v = 2 m/min and varying both the laser power and the laser spot diameter, it can be observed that when the spot diameter is greater than 2.5 mm and the laser power is below 260 W, the surface hardness of the material remains almost unchanged compared with the original hardness of the base material. In contrast, when the laser power exceeds 260 W and the laser spot diameter is smaller than 2.5 mm, the surface hardness of the material increases significantly, following the principle that a higher laser power combined with a smaller spot diameter produces higher surface hardness, while the opposite conditions yield a lower hardness. Among these two factors, the laser spot diameter exerts a stronger influence on surface hardness than the laser power, as illustrated in Figure 11. This can be explained by the fact that a larger spot diameter reduces the power density delivered to the material, thereby lowering the laser's thermal effect on the surface. Overall, the results emphasize the importance of carefully selecting both parameters, with particular attention to the spot diameter, to optimize the hardness characteristics of laser-treated materials.

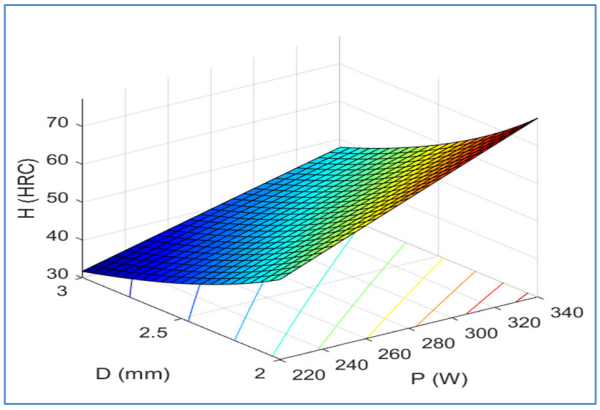

Fig. 11. Effect of P and D on the surface hardness of the part.

The effects of the laser head speed and the laser spot diameter on the surface hardness of the part are: With the laser power set to a constant value of P = 280 W, the diameter of the laser spot on the part surface and the laser head speed were varied. The results show that with a spot diameter (D) smaller than 2.5mm and a laser head speed (v) lower than 2 m/min, the surface hardness of the part changes according to the principle that as the laser spot diameter and the laser head speed decrease, the surface hardness of the part increases. Among these factors, the effect of the laser spot diameter on the surface hardness of the part is greater than that of the laser head speed, as depicted in Figure 12.

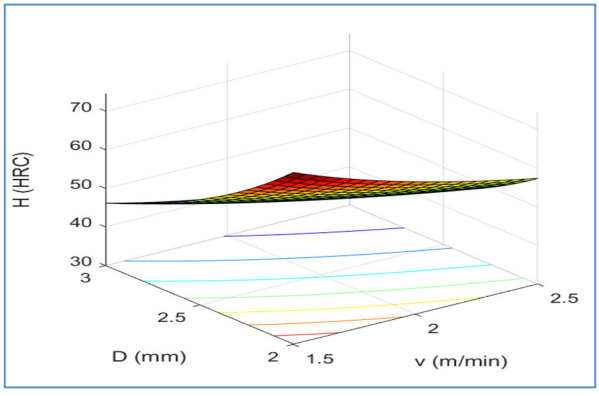

Fig. 12. The effect of v and D on the surface hardness of the part.

Using MINITAB software to analyze the mathematical model (2), it was found that the laser spot diameter had the most significant impact on surface hardness (42.8%). Accordingly, increasing the laser spot diameter resulted in a decrease in surface hardness, and vice versa. Next, the laser power had a greater effect on surface hardness (31.4%) compared to the laser head speed, which accounted for 25.4%.

IV. CONCLUSIONS

This study has delivered significant insights into optimizing the process parameters for LHT of 9XC steel. By maintaining a constant laser spot diameter (D = 2.5 mm) and laser head speed (v = 1.5 m/min), and varying the laser power from 180 W to 340 W, it was confirmed that low power levels (e.g., 180 W) produce surface temperatures insufficient for austenite transformation, highlighting the need for higher power to achieve effective hardening. The experimental results revealed a correlation between the laser head speed and surface temperature, where increasing the travel speed led to a noticeable reduction in surface temperature. Among all investigated parameters, the laser spot diameter had the most significant effect on surface temperature, followed by laser power and head speed. Moreover, the analysis showed that surface hardness was predominantly influenced by the laser spot diameter (42.8%), with lesser contributions from the laser power (31.4%) and head speed (25.4%). Larger spot diameters consistently produced lower surface hardness values, underscoring the importance of the power density in achieving effective surface hardening. These findings not only provide a pathway to improve the machining productivity by adjusting the head speed without significantly compromising the surface temperature but also establish a mathematical model that enables a fast and reliable selection of process parameters. This model serves as a practical tool for both industry and research, ensuring consistent product quality while reducing experimental effort. Ultimately, this work lays a strong foundation for future investigations into parameter optimization for advanced laser-based manufacturing.

REFERENCES

[1] J. C. Rozzi, F. E. Pfefferkorn, F. P. Incropera, and Y. C. Shin, "Transient, three-dimensional heat transfer model for the laser assisted machining of silicon nitride: I. Comparison of predictions with measured surface temperature histories," *International Journal of Heat and Mass Transfer*, vol. 43, no. 8, pp. 1409–1424, Apr. 2000, https://doi.org/10.1016/S0017-9310(99)00217-3.

[2] S. Lei, Y. C. Shin, and F. P. Incropera, "Experimental Investigation of Thermo-Mechanical Characteristics in Laser-Assisted Machining of Silicon Nitride Ceramics," *Journal of Manufacturing Science and Engineering*, vol. 123, no. 4, pp. 639–646, Oct. 2000, https://doi.org/10.1115/1.1380382.

[3] F. E. Pfefferkorn, Y. C. Shin, Y. Tian, and F. P. Incropera, "Laser-Assisted Machining of Magnesia-Partially-Stabilized Zirconia," *Journal of Manufacturing Science and Engineering*, vol. 126, no. 1, pp. 42–51, Mar. 2004, https://doi.org/10.1115/1.1644542.

[4] Y. Wang, L. J. Yang, and N. J. Wang, "An investigation of laser-assisted machining of Al2O3 particle reinforced aluminum matrix composite," *Journal of Materials Processing Technology*, vol. 129, no. 1, pp. 268–272, Oct. 2002, https://doi.org/10.1016/S0924-0136(02)00616-7.

[5] H. Ding and Y. C. Shin, "Improvement of machinability of Waspaloy via laser-assisted machining," *The International Journal of Advanced Manufacturing Technology*, vol. 64, no. 1, pp. 475–486, Jan. 2013, https://doi.org/10.1007/s00170-012-4012-8.

[6] S. Rajagopal, D. J. Plankenhorn, and V. L. Hill, "Machining aerospace alloys with the aid of a 15 kW laser," *Journal of Applied Metalworking*, vol. 2, no. 3, pp. 170–184, July 1982, https://doi.org/10.1007/BF02834035.

[7] M. Anderson, R. Patwa, and Y. C. Shin, "Laser-assisted machining of Inconel 718 with an economic analysis," *International Journal of Machine Tools and Manufacture*, vol. 46, no. 14, pp. 1879–1891, Nov. 2006, https://doi.org/10.1016/j.ijmachtools.2005.11.005.

[8] J. C. Rozzi, F. E. Pfefferkorn, F. P. Incropera, and Y. C. Shin, "Transient Thermal Response of a Rotating Cylindrical Silicon Nitride Workpiece Subjected to a Translating Laser Heat Source, Part I: Comparison of Surface Temperature Measurements With Theoretical Results," *Journal of Heat Transfer*, vol. 120, no. 4, pp. 899–906, Nov. 1998, https://doi.org/10.1115/1.2825909.

[9] V. Garcí;a Navas, I. Arriola, O. Gonzalo, and J. Leunda, "Mechanisms involved in the improvement of Inconel 718 machinability by laser assisted machining (LAM)," *International Journal of Machine Tools and Manufacture*, vol. 74, pp. 19–28, Nov. 2013, https://doi.org/10.1016/j.ijmachtools.2013.06.009.

[10] P. Dumitrescu, P. Koshy, J. Stenekes, and M. A. Elbestawi, "High-power diode laser assisted hard turning of AISI D2 tool steel," *International Journal of Machine Tools and Manufacture*, vol. 46, no. 15, pp. 2009–2016, Dec. 2006, https://doi.org/10.1016/j.ijmachtools.2006.01.005.

[11] S. Skvarenina and Y. C. Shin, "Laser-assisted machining of compacted graphite iron," *International Journal of Machine Tools and Manufacture*, vol. 46, no. 1, pp. 7–17, Jan. 2006, https://doi.org/10.1016/j.ijmachtools.2005.04.013.

[12] H. Ding and Y. C. Shin, "Laser-assisted machining of hardened steel parts with surface integrity analysis," *International Journal of Machine Tools and Manufacture*, vol. 50, no. 1, pp. 106–114, Jan. 2010, https://doi.org/10.1016/j.ijmachtools.2009.09.001.

[13] S. H. Masood, K. Armitage, and M. Brandt, "An experimental study of laser-assisted machining of hard-to-wear white cast iron," *International Journal of Machine Tools and Manufacture*, vol. 51, no. 6, pp. 450–456, June 2011, https://doi.org/10.1016/j.ijmachtools.2011.02.001.

[14] T-H Nguyen and N. Duc-Toan, "Experimental Researches of Turning Hardened 9CrSi Alloy Tool Steel with Laser-Assisted Machining," *Arabian Journal for Science and Engineering*, vol. 46, no. 12, pp. 11725–11738, Dec. 2021, https://doi.org/10.1007/s13369-021-05685-6.

[15] S. Sun, M. Brandt, and M. S. Dargusch, "Thermally enhanced machining of hard-to-machine materials—A review," *International Journal of Machine Tools and Manufacture*, vol. 50, no. 8, pp. 663–680, Aug. 2010, https://doi.org/10.1016/j.ijmachtools.2010.04.008.

[16] W. M. Steen and J. Mazumder, *Laser Material Processing*. Springer Science & Business Media, 2010.

[17] E. Kennedy, G. Byrne, and D. N. Collins, "A review of the use of high power diode lasers in surface hardening," *Journal of Materials Processing Technology*, vol. 155–156, pp. 1855–1860, Nov. 2004, https://doi.org/10.1016/j.jmatprotec.2004.04.276.

[18] J. Rana, G. L. Goswami, S. K. Jha, P. K. Mishra, and B. V. S. S. S. Prasad, "Experimental studies on the microstructure and hardness of laser-treated steel specimens," *Optics & Laser Technology*, vol. 39, no. 2, pp. 385–393, Mar. 2007, https://doi.org/10.1016/j.optlastec.2005.07.001.

[19] D. Schuocker, *High Power Lasers In Production Engineering*. World Scientific Publishing Company, 1999.

[20] *Heat Treating Progress The Official Voice of the ASM Heat Treating Society*. USA: ASM International, 2005.

[21] *Heat treating with lasers*. USA: ASM International, 1998.

[22] J. Mazumder and W. M. Steen, "Heat transfer model for cw laser material processing," *Journal of Applied Physics*, vol. 51, no. 2, pp. 941–947, Feb. 1980, https://doi.org/10.1063/1.327672.

[23] J. Hannweber, S. Bonss, B. Brenner, and E. Beyer, "Integrated laser system for heat treatment with high power diode laser," presented at the ICALEO 2004: 23rd International Congress on Laser Materials Processing and Laser Microfabrication, Oct. 2004, https://doi.org/10.2351/1.5060221.

[24] T. H. Nguyen, D. T. Nguyen, V. H. Tran, and V. M. Nguyen, "Research the Influence of Technological Parameters on the Hardness of Detail When Surface Hardening of Steel 9XC by Laser ND:YAG," in *Proceedings of the 3rd Annual International Conference on Material, Machines and Methods for Sustainable Development (MMMS2022)*, Cham, 2024, pp. 107–114, https://doi.org/10.1007/978-3-031-39090-6_12.

[25] M. I. Mohamed, "Studies of the Properties and Microstructure of Heat Treated 0.27% C and 0.84% Mn Steel," *Engineering, Technology & Applied Science Research*, vol. 8, no. 5, pp. 3484–3487, Oct. 2018, https://doi.org/10.48084/etasr.2065.